

**Black Holes in the Dilatonic Einstein-Gauss-Bonnet Theory in  
Various Dimensions III**  
– Asymptotically AdS Black Holes with  $k = \pm 1$  –

Nobuyoshi OHTA<sup>a,\*</sup>) and Takashi TORII<sup>b,\*\*</sup>)

<sup>a</sup>*Department of Physics, Kinki University, Higashi-Osaka, Osaka 577-8502,  
Japan*

<sup>b</sup>*Department of General Education, Osaka Institute of Technology,  
Asahi-ku, Osaka 535-8585, Japan*

**Abstract**

We study black hole solutions in the Einstein-Gauss-Bonnet gravity with the dilaton and a negative “cosmological constant”. We derive the field equations for the static spherically symmetric ( $k = 1$ ) and hyperbolically symmetric ( $k = -1$ ) spacetime in general  $D$  dimensions. The system has some scaling symmetries which are used in our analysis of the solutions. We find exact solutions, i.e., regular AdS solution for  $k = 1$  and a massless black hole solution for  $k = -1$ . Nontrivial asymptotically AdS solutions are obtained numerically in  $D = 4 - 6$  and 10 dimensional spacetimes. For spherically symmetric solutions, there is the minimum horizon radius below which no solution exists in  $D = 4 - 6$ . However in  $D = 10$ , there is not such lower bound but the solution continues to exist to zero horizon size. For hyperbolically symmetric solution, there is the minimum horizon radius in all dimensions. Our solution can be used for investigations of the boundary theory through AdS/CFT correspondence.

---

<sup>\*</sup>) e-mail address: ohtan at phys.kindai.ac.jp

<sup>\*\*</sup>) e-mail address: torii at ge.oit.ac.jp

## §1. Introduction

This is the third of the series of our papers about the black hole solutions in dilatonic Einstein-Gauss-Bonnet theory in higher dimensions.<sup>1),2)</sup>

Many works have been done on black hole solutions in dilatonic gravity, and various properties have been studied since the works in Refs. 3) and 4). It was found that the dilaton modifies the properties of the black hole solution. On the other hand, it is known that there are higher-order corrections from string theories.<sup>5)</sup> It is then natural to ask how these corrections may modify the results. Several works have studied the effects of higher order terms,<sup>6)-10)</sup> but most of the work done so far considers theories without dilaton,<sup>11)-13)</sup> which is one of the most important ingredients in the string effective theories. Hence it is important to study black hole solutions and their properties in the theory with both the higher order corrections and dilaton. The simplest higher order correction is the Gauss-Bonnet (GB) term, which may appear in heterotic string theories.

In the first paper in this series,<sup>1)</sup> we focused on asymptotically flat solutions and studied system with the GB correction term and dilaton without the cosmological term in various dimensions from 4 to 10. They are spherically symmetric with the  $(D - 2)$ -dimensional hypersurface of curvature signature  $k = 1$ . We have then turned to planer symmetric ( $k = 0$ ) topological black holes, but have found that no solution exists without the cosmological term. In the string perspective, it is more interesting to examine asymptotically anti-de Sitter (AdS) black hole solutions with possible application to AdS/CFT correspondence in mind. Discussions of the origin of such cosmological terms are given in Refs. 14), 15). So in the second paper in this series,<sup>2)</sup> we have presented the results on black hole solutions with a negative cosmological term with  $k = 0$ . In fact, shear viscosity has been computed using the result in our previous paper.<sup>16)</sup>

In this paper, we extend our previous work to solutions with  $k = \pm 1$  and a negative cosmological term. Black hole solutions in dilatonic Einstein-Maxwell theories with Liouville-type potential but without GB term are studied in Refs. 17), 18). Exact solutions and their properties are discussed in Ref. 19) in dilatonic Einstein theory with Liouville potential. Cosmological solutions are also considered in Ref. 20). The presence of a Liouville potential already changes completely the difficulty of the system. In fact it is no longer an integrable system even in the absence of a GB term and our system is far much difficult one. Nevertheless, we find some exact solutions in our complicated system of Einstein-GB system with a dilaton. These are the regular AdS solution for  $k = 1$  and a massless black hole solution for  $k = -1$ . We also obtain nontrivial asymptotically AdS solutions numerically in  $D = 4 - 6$  and 10 dimensional spacetimes and discuss their properties. We expect that these solutions

should be useful for studying properties of dual field theories.

This paper is organized as follows. In § 2, we first present the action and give basic equations to solve. Symmetry properties of the theory are also discussed in order to apply them in our following analysis. In § 3, boundary conditions at the horizon and relevant asymptotic behaviors are examined. In § 4 and § 5, we first give the exact solutions of the regular AdS solution for  $k = 1$  and a massless black hole solution for  $k = -1$ , and then present our numerical solutions in  $D = 4 - 6$  and 10 for  $k = +1$  and  $k = -1$ , respectively. These solutions are presented for a particular choice of the parameters in our theory, but we expect that the qualitative behaviors do not change for other choices though the range of the horizon radii for the existence of the black hole solutions seems to change depending on the strength of the dilaton coupling  $\gamma$ . Some discussions on this problem as well as on the difference between string frame and Einstein frame is given in Ref. 21) for asymptotically flat solutions without cosmological term. § 6 is devoted to conclusions and discussions.

## §2. Dilatonic Einstein-Gauss-Bonnet theory

### 2.1. Action and basic equations

We consider the following low-energy effective action for a heterotic string

$$S = \frac{1}{2\kappa_D^2} \int d^D x \sqrt{-g} \left[ R - \frac{1}{2}(\partial_\mu \phi)^2 + \alpha_2 e^{-\gamma\phi} R_{\text{GB}}^2 - \Lambda e^{\lambda\phi} \right], \quad (2.1)$$

where  $\kappa_D^2$  is a  $D$ -dimensional gravitational constant,  $\phi$  is a dilaton field,  $\alpha_2 = \alpha'/8$  is a numerical coefficient given in terms of the Regge slope parameter, and  $R_{\text{GB}}^2 = R_{\mu\nu\rho\sigma} R^{\mu\nu\rho\sigma} - 4R_{\mu\nu} R^{\mu\nu} + R^2$  is the GB correction. We leave the coupling constant of dilaton  $\gamma$  arbitrary as much as possible, while the ten-dimensional critical string theory predicts  $\gamma = 1/2$ . Since the negative cosmological constant  $\Lambda = -(D-1)(D-2)/\ell^2$  couples to the dilaton with the coupling constant  $\lambda$ , this term can be regarded as the potential of the dilaton. If this is the only potential, there is no stationary point and the dilaton cannot have a stable asymptotic value. However, for asymptotically AdS solutions, the Gauss-Bonnet term produces an additional potential in the asymptotic region, and the dilaton can take finite constant value at infinity. There may be several possible sources of “cosmological terms” with different dilaton couplings, so we leave  $\lambda$  arbitrary and specify it in the numerical analysis.

Varying the action (2.1) with respect to  $g_{\mu\nu}$ , we obtain the gravitational equation:

$$G_{\mu\nu} - \frac{1}{2} \left[ \nabla_\mu \phi \nabla_\nu \phi - \frac{1}{2} g_{\mu\nu} (\nabla\phi)^2 \right] + \frac{1}{2} g_{\mu\nu} \Lambda e^{\lambda\phi} + \alpha_2 e^{-\gamma\phi} \left[ H_{\mu\nu} + 4(\gamma^2 \nabla^\rho \phi \nabla^\sigma \phi - \gamma \nabla^\rho \nabla^\sigma \phi) P_{\mu\rho\nu\sigma} \right] = 0, \quad (2.2)$$

where

$$G_{\mu\nu} \equiv R_{\mu\nu} - \frac{1}{2}g_{\mu\nu}R, \quad (2.3)$$

$$H_{\mu\nu} \equiv 2(RR_{\mu\nu} - 2R_{\mu\rho}R^\rho{}_\nu - 2R^{\rho\sigma}R_{\mu\rho\nu\sigma} + R_\mu{}^{\rho\sigma\lambda}R_{\nu\rho\sigma\lambda}) - \frac{1}{2}g_{\mu\nu}R_{\text{GB}}^2, \quad (2.4)$$

$$P_{\mu\nu\rho\sigma} \equiv R_{\mu\nu\rho\sigma} + 2g_{\mu[\sigma}R_{\rho]\nu} + 2g_{\nu[\rho}R_{\sigma]\mu} + Rg_{\mu[\rho}g_{\sigma]\nu}. \quad (2.5)$$

$P_{\mu\nu\rho\sigma}$  is the divergence free part of the Riemann tensor, i.e.  $\nabla_\mu P^\mu{}_{\nu\rho\sigma} = 0$ . The equation of the dilaton field is

$$\square\phi - \alpha_2\gamma e^{-\gamma\phi}R_{\text{GB}}^2 - \lambda\Lambda e^{\lambda\phi} = 0, \quad (2.6)$$

where  $\square$  is the  $D$ -dimensional d'Alembertian.

We parametrize the metric as

$$ds_D^2 = -Be^{-2\delta}dt^2 + B^{-1}dr^2 + r^2h_{ij}dx^i dx^j, \quad (2.7)$$

where  $h_{ij}dx^i dx^j$  represents the line element of a  $(D-2)$ -dimensional hypersurface with constant curvature  $(D-2)(D-3)k$  and volume  $\Sigma_k$  for  $k = \pm 1, 0$ .

The metric function  $B = B(r)$  and the lapse function  $\delta = \delta(r)$  depend only on the radial coordinate  $r$ . The field equations are<sup>2)</sup>

$$\begin{aligned} & [(k-B)\tilde{r}^{D-3}]' \frac{D-2}{\tilde{r}^{D-4}} h - \frac{1}{2}B\tilde{r}^2\phi'^2 - (D-1)_4 e^{-\gamma\phi} \frac{(k-B)^2}{\tilde{r}^2} \\ & + 4(D-2)_3 \gamma e^{-\gamma\phi} B(k-B)(\phi'' - \gamma\phi'^2) \\ & + 2(D-2)_3 \gamma e^{-\gamma\phi} \phi' \frac{(k-B)[(D-3)k - (D-1)B]}{\tilde{r}} - \tilde{r}^2 \tilde{\Lambda} e^{\lambda\phi} = 0, \end{aligned} \quad (2.8)$$

$$\delta'(D-2)\tilde{r}h + \frac{1}{2}\tilde{r}^2\phi'^2 - 2(D-2)_3 \gamma e^{-\gamma\phi} (k-B)(\phi'' - \gamma\phi'^2) = 0, \quad (2.9)$$

$$\begin{aligned} (e^{-\delta}\tilde{r}^{D-2}B\phi')' &= \gamma(D-2)_3 e^{-\gamma\phi-\delta}\tilde{r}^{D-4} \left[ (D-4)_5 \frac{(k-B)^2}{\tilde{r}^2} + 2(B' - 2\delta'B)B' \right. \\ & \left. - 4(k-B)BU(r) - 4\frac{D-4}{\tilde{r}}(B' - \delta'B)(k-B) \right] + e^{-\delta}\tilde{r}^{D-2}\lambda\tilde{\Lambda}e^{\lambda\phi}, \end{aligned} \quad (2.10)$$

where  $\tilde{r} \equiv r/\sqrt{\alpha_2}$ ,  $\tilde{\Lambda} = \alpha_2\Lambda$  are the dimensionless variables, and the primes in the field equations denote the derivatives with respect to  $\tilde{r}$ . Other functions are defined as

$$\begin{aligned} (D-m)_n &\equiv (D-m)(D-m-1)(D-m-2)\cdots(D-n), \\ h &\equiv 1 + 2(D-3)e^{-\gamma\phi} \left[ (D-4)\frac{k-B}{\tilde{r}^2} + \gamma\phi' \frac{3B-k}{\tilde{r}} \right], \end{aligned} \quad (2.11)$$

$$\tilde{h} \equiv 1 + 2(D-3)e^{-\gamma\phi} \left[ (D-4)\frac{k-B}{\tilde{r}^2} + \gamma\phi' \frac{2B}{\tilde{r}} \right], \quad (2.12)$$

$$\begin{aligned}
U(r) \equiv (2\tilde{h})^{-1} & \left[ (D-3)_4 \frac{k-B}{\tilde{r}^2 B} - 2 \frac{D-3}{\tilde{r}} \left( \frac{B'}{B} - \delta' \right) - \frac{1}{2} \phi'^2 \right. \\
& + (D-3) e^{-\gamma\phi} \left\{ (D-4)_6 \frac{(k-B)^2}{\tilde{r}^4 B} - 4(D-4)_5 \frac{k-B}{\tilde{r}^3} \left( \frac{B'}{B} - \delta' - \gamma\phi' \right) \right. \\
& - 4(D-4)\gamma \frac{k-B}{\tilde{r}^2} \left( \gamma\phi'^2 + \frac{D-2}{\tilde{r}} \phi' - \Phi \right) \\
& + 8 \frac{\gamma\phi'}{\tilde{r}} \left[ \left( \frac{B'}{2} - \delta' B \right) \left( \gamma\phi' - \delta' + \frac{2}{\tilde{r}} \right) - \frac{D-4}{2\tilde{r}} B' \right] \\
& \left. \left. + 4(D-4) \left( \frac{B'}{2B} - \delta' \right) \frac{B'}{\tilde{r}^2} - \frac{4\gamma}{\tilde{r}} \Phi (B' - 2\delta' B) \right\} - \frac{1}{B} \tilde{\Lambda} e^{\lambda\phi} \right], \tag{2.13}
\end{aligned}$$

$$\Phi \equiv \phi'' + \left( \frac{B'}{B} - \delta' + \frac{D-2}{\tilde{r}} \right) \phi'. \tag{2.14}$$

## 2.2. Symmetry and scaling

Our field equations has several scaling symmetries. Firstly the field equations are invariant under the transformation:

$$\gamma \rightarrow -\gamma, \quad \lambda \rightarrow -\lambda, \quad \phi \rightarrow -\phi. \tag{2.15}$$

By this symmetry, we can restrict the parameter range of  $\gamma$  to  $\gamma \geq 0$ . The second one is the shift symmetry:

$$\phi \rightarrow \phi - \phi_*, \quad \tilde{\Lambda} \rightarrow e^{(\lambda-\gamma)\phi_*} \tilde{\Lambda}, \quad r \rightarrow e^{-\gamma\phi_*/2} r. \tag{2.16}$$

where  $\phi_*$  is an arbitrary constant. This may be used to generate solutions for different cosmological constants, given a solution for some cosmological constant and  $\tilde{r}_H$ . Details will be discussed in § 4. The final one is the shift symmetry under

$$\delta \rightarrow \delta - \delta_*, \quad t \rightarrow e^{-\delta_*} t, \tag{2.17}$$

with an arbitrary constant  $\delta_*$ , which may be used to shift the asymptotic value of  $\delta$  to zero.

The model (2.1) has several parameters of the theory such as  $D$ ,  $\alpha_2$ ,  $\Lambda$ ,  $\gamma$ , and  $\lambda$ . The black hole solutions have also physical parameters such as the horizon radius  $\tilde{r}_H$  and the value of  $\delta$  at infinity. However owing to the above symmetries (including the scaling by  $\alpha_2$ ), we can reduce the number of the parameters and are left only with  $D$ ,  $\gamma \geq 0$ ,  $\lambda$ , and  $\tilde{r}_H$ .

## §3. Boundary conditions and asymptotic behavior

In the numerical search for the appropriate black hole solutions, we should impose the conditions that they have the regular event horizons and outer spacetimes should be singularity free. As for the asymptotic structure, we assume AdS like spacetime. Let us now examine them in detail.

### 3.1. Regular horizon

We impose the following boundary conditions for the metric functions:

1. The existence of a regular horizon  $\tilde{r}_H$ :

$$B(\tilde{r}_H) = 0, \quad |\delta_H| < \infty, \quad |\phi_H| < \infty. \quad (3.1)$$

2. The nonexistence of singularities outside the event horizon ( $\tilde{r} > \tilde{r}_H$ ):

$$B(\tilde{r}) > 0, \quad |\delta| < \infty, \quad |\phi| < \infty. \quad (3.2)$$

Here and in what follows, the values of various quantities at the horizon are denoted with subscript  $H$ . At the horizon, it follows from Eqs. (2.8), (2.11), and (2.12) that

$$\begin{aligned} B_H &= 0, \\ h_H &= 1 + 2(D-3)k \frac{e^{-\gamma\phi_H}}{\tilde{r}_H^2} [D-4 - \gamma\phi'_H \tilde{r}_H], \\ \tilde{h}_H &= 1 + 2(D-3)_4 k \frac{e^{-\gamma\phi_H}}{\tilde{r}_H^2}, \\ B'_H h_H &= \frac{(D-3)k}{\tilde{r}_H} + \frac{(D-3)_5 k^2}{\tilde{r}_H^2} e^{-\gamma\phi_H} - \tilde{r}_H \frac{\tilde{\Lambda} e^{\lambda\phi_H}}{D-2}. \end{aligned} \quad (3.3)$$

Using these in Eq. (2.10) gives

$$\begin{aligned} & 2kC\gamma \left[ -2L\tilde{r}_H^2 \left\{ 1 + kC[D-4 - (D-2)\gamma\lambda] + (D-2)k^2C^2\gamma[(D-6)\gamma - (D-4)\lambda] \right\} \right. \\ & \quad \left. + (D-2)k \left\{ 2(D-3) + (D-4)(3D-11)kC \right. \right. \\ & \quad \left. \left. + (D-4)k^2C^2[(D-2)(3D-11)\gamma^2 + (D-4)_5] + 2(D-2)_5 k^3 C^3 \gamma^2 \right\} \right] \tilde{r}_H^2 \phi_H^2 \\ & + 2 \left[ 4k^2C^2\gamma^2 L^2 \tilde{r}_H^4 + 2L\tilde{r}_H^2 \left\{ 1 + 2kC[D-4 - (D-2)\gamma\lambda] \right. \right. \\ & \quad \left. \left. - k^2C^2[2(D-2)(2D-5)\gamma^2 + 4(D-2)(D-4)\gamma\lambda - (D-4)^2] \right. \right. \\ & \quad \left. \left. - 2(D-2)(D-4)k^3C^3\gamma[(D-2)\gamma + (D-4)\lambda] \right\} \right. \\ & \quad \left. + (D-2)k \left\{ (D-1)_2(D-4)k^2C^2\gamma^2[2 + 2kC - (D-4)_5 k^2 C^2] \right. \right. \\ & \quad \left. \left. - [1 + (D-4)kC]^2 [2(D-3) + (D-4)_5 kC] \right\} \right] \tilde{r}_H \phi'_H \\ & + 4C\gamma L^2 \tilde{r}_H^4 + 4(D-2)L\tilde{r}_H^2 \left\{ \lambda[1 + (D-4)kC]^3 \right. \\ & \quad \left. + kC\gamma[D(D-4)^2 k^2 C^2 + (D-4)(D+1)kC - (D-2)] \right\} \\ & \left. + (D-1)_2(D-2)k^2C\gamma \left\{ 2(D-2) - 4(D-4)kC - (D-4)^2(D+1)k^2C^2 \right\} = 0, \quad (3.4) \end{aligned}$$

where we have defined

$$C = \frac{2(D-3)e^{-\gamma\phi_H}}{\tilde{r}_H^2}, \quad L = e^{\lambda\phi_H}\tilde{\Lambda}. \quad (3.5)$$

Eq. (3.4) is a quadratic equation to determine  $\phi'_H$  and there can be solutions only if we have real solutions in this equation. We will see that this gives strong constraint on our solutions.

### 3.2. Asymptotic behavior at infinity

At infinity we impose the condition that the leading term of the metric function  $B$  comes from AdS radius, i.e.,

3. “AdS asymptotic behavior” ( $\tilde{r} \rightarrow \infty$ ):

$$B \sim \tilde{b}_2\tilde{r}^2 + k - \frac{2\tilde{M}}{\tilde{r}^\mu}, \quad \delta(r) \sim \delta_0 + \frac{\delta_1}{\tilde{r}^\sigma}, \quad \phi \sim \phi_0 + \frac{\phi_1}{\tilde{r}^\nu}, \quad (3.6)$$

with finite constants  $\tilde{b}_2 > 0$ ,  $\tilde{M}$ ,  $\delta_0$ ,  $\delta_1$ ,  $\phi_0$ ,  $\phi_1$  and positive constant  $\mu$ ,  $\sigma$ ,  $\nu$ .

The coefficient of the first term  $\tilde{b}_2$  is related to the AdS radius as  $\tilde{b}_2 = \tilde{\ell}_{\text{AdS}}^{-2}$ . However, this condition is not sufficient for the spacetime to be AdS asymptotically. Strictly speaking, asymptotically AdS spacetime is left invariant under  $SO(D-1, 2)$ .<sup>22)</sup> Whether the solution satisfies the AdS-invariant boundary condition or not depends on the value of the power indices  $\mu$ ,  $\sigma$ ,  $\nu$ .

Substituting Eqs. (3.6) into the field equations (2.8) and (2.10), one finds the leading terms ( $\tilde{r}^2$  and constant terms in each equation) give the conditions

$$(D)_{3\gamma} e^{-\gamma\phi_0}\tilde{b}_2^2 + \lambda\tilde{\Lambda}e^{\lambda\phi_0} = 0, \quad (3.7)$$

$$(D-1)_4 e^{-\gamma\phi_0}\tilde{b}_2^2 - (D-1)_2\tilde{b}_2 - \tilde{\Lambda}e^{\lambda\phi_0} = 0, \quad (3.8)$$

which determine  $\tilde{b}_2$  and  $\phi_0$ , while  $\delta_0$  can be arbitrary because only its derivative appears in the field equations. We can restrict the parameter to  $\lambda > 0$  by Eq. (3.7) and assume  $\lambda \neq \gamma$ . Then, Eqs. (3.7) and (3.8) give

$$\tilde{b}_2^2 = \frac{-\lambda\tilde{\Lambda}}{(D)_{3\gamma}} \left[ \frac{D(D-3)}{(D-1)_2} (-\tilde{\Lambda}) \frac{\gamma}{\lambda} \left( 1 + \frac{(D-4)\lambda}{D\gamma} \right)^2 \right]^{\frac{\gamma+\lambda}{\gamma-\lambda}}, \quad (3.9)$$

$$e^{\phi_0} = \left[ \frac{D(D-3)}{(D-1)_2} (-\tilde{\Lambda}) \frac{\gamma}{\lambda} \left( 1 + \frac{(D-4)\lambda}{D\gamma} \right)^2 \right]^{\frac{1}{\gamma-\lambda}}. \quad (3.10)$$

The candidates of the next leading terms are almost the same as those in  $k = 0$  case except for some additional terms which are proportional to  $k$ . However, these additional terms turn out to be further subleading ones by detailed analysis. This means that the

asymptotic behaviors are the same as in the  $k = 0$  case, which is discussed in our previous paper.<sup>2)</sup> Hence we only summarize the results here without details.

We consider the case with  $(D - 4)\lambda - D\gamma \neq 0$ . There are two different classes which give consistent expansions. One is  $\mu = D - 3$  and  $\nu, \sigma > D - 1$ , and we rename the coefficient  $\tilde{M}$  as  $\tilde{M}_0$ .

The other class is  $\mu = \nu - 2 = \sigma - 2$  and

$$\nu = \nu_{\pm} \equiv \frac{D - 1}{2} \left[ 1 \pm \sqrt{1 - \frac{4(D)_2 \lambda \gamma (\lambda - \gamma) [(D - 4)\lambda + D\gamma]}{(D - 1)^2 [(D - 4)^2 \lambda^2 - D^2 \gamma^2 - 8(D - 1)_2 \lambda^2 \gamma^2]}} \right]. \quad (3.11)$$

The asymptotic forms of the fields are then

$$\begin{aligned} \phi &\sim \phi_0 + \frac{\phi_+}{\tilde{r}^{\nu_+}} + \dots, \\ B &\sim \tilde{b}_2 \tilde{r}^2 + k - \frac{2\tilde{M}_+}{\tilde{r}^{\nu_+ - 2}} - \frac{2\tilde{M}_0}{\tilde{r}^{D - 3}} + \dots, \\ \delta &\sim \frac{\delta_+}{\tilde{r}^{\nu_+}} + \dots. \end{aligned} \quad (3.12)$$

There will be in general  $\phi_-/\tilde{r}^{\nu_-}$  term in the asymptotic behavior of  $\phi$ , but we tune the boundary condition of  $\phi_H$  to kill this term. Note that while  $B$  has the term  $\tilde{r}^{-\nu_+ + 2}$ , the  $g_{tt}$  component of the metric behaves as

$$-g_{tt} = B e^{-2\delta} \sim \tilde{b}_2 \tilde{r}^2 + k - \frac{2\tilde{M}_0}{\tilde{r}^{D - 3}} + \dots. \quad (3.13)$$

This value of  $\tilde{M}_0$  is the gravitational mass of the black holes. Thus it is convenient to define the mass function  $\tilde{m}_g(\tilde{r})$  by

$$-g_{tt} = \tilde{b}_2 \tilde{r}^2 + k - \frac{2\tilde{m}_g(\tilde{r})}{\tilde{r}^{D - 3}}. \quad (3.14)$$

We will present our results in terms of this function.

### 3.3. Allowed parameter regions

As in our previous paper,<sup>2)</sup> imposing the conditions

$$\tilde{m}_{BF}^2 \leq \tilde{m}^2, \quad \tilde{m}^2 < 0, \quad (3.15)$$

where<sup>23), 24)</sup>

$$\tilde{m}_{BF}^2 = -\frac{(D - 1)^2}{4\tilde{\ell}_{AdS}^2} = -\frac{(D - 1)^2}{4} \tilde{b}_2, \quad (3.16)$$

we get the allowed regions of our parameters  $(\lambda, \gamma)$  for the existence of asymptotically AdS solutions. Because these are the same as in our previous paper,<sup>2)</sup> we refer the reader to that paper for the explicit regions.



#### §4. Spherically symmetric black hole solutions with $k = 1$

We construct our black hole solutions numerically for the parameters

$$\gamma = \frac{1}{2}, \quad \lambda = \frac{1}{3}, \quad \tilde{\Lambda} = -1, \quad (4.1)$$

and the conditions

$$\phi_- = 0, \quad \delta_0 = 0, \quad (4.2)$$

in  $D = 4 - 6$  and 10.

We integrate the field equations from the event horizon to infinity. The first step in the procedure is to choose appropriate radius of the event horizon  $\tilde{r}_H$ . We find that we should choose large radius in this process, for instance  $\tilde{r}_H \sim 100$ , because there are cases where no solution exists for small horizon radii. Next we choose the value of  $\phi_H$  and determine the values of other fields by Eqs. (3.3) and (3.4). Since the condition (4.2) is in general not satisfied for most of the values  $\phi_H$ , it should be tuned such that  $\phi_- = 0$  is achieved in the asymptotic behavior (3.12). We also fix  $\delta_H = 0$  in the integration and this would give nonzero  $\delta_0$ . However  $\delta_0 = 0$  is always realized by the shift symmetry (2.17) so we do not have to worry about that. As a result, there is only one freedom of choosing  $\tilde{r}_H$ , given a cosmological constant. The solutions are obtained for the particular choice of  $\gamma$  and  $\lambda$ , but we expect that qualitative properties do not change for other choices of these parameters, though there is an indication that the range of the horizon radii for the existence of the black hole solutions changes depending on the strength of the dilaton coupling  $\gamma$ .<sup>21)</sup> Using the symmetry in Eq. (2.16), the solutions for different values of cosmological constant can be generated from a solution for  $\tilde{\Lambda} = -1$ . Indeed, solutions for  $\tilde{\Lambda}_1$  can be obtained by simply changing the variables as

$$\tilde{r} \rightarrow |\tilde{\Lambda}_1|^{-\frac{\gamma}{2(\lambda-\gamma)}} \tilde{r}, \quad \phi \rightarrow \phi - \frac{1}{\lambda - \gamma} \log |\tilde{\Lambda}_1|, \quad \tilde{m}_g \rightarrow |\tilde{\Lambda}_1|^{-\frac{(D-3)\gamma}{2(\lambda-\gamma)}} \tilde{m}_g. \quad (4.3)$$

Let us examine the boundary condition (3.4) in more detail here. It is a quadratic equation with respect to  $\phi'_H$ . To guarantee the reality of  $\phi'_H$ , we find that there are forbidden parameter regions for  $\tilde{r}_H$  and  $\phi_H$ . Such regions (or allowed regions) are depicted in Fig. 1 for our choice of parameters  $\gamma$ ,  $\lambda$  and  $\tilde{\Lambda}$  in each dimension. The solutions can exist only in those shaded regions. However, this does not mean that there are always solutions for those values in these regions. We also mention that the regions seem to change depending on the parameter choice of  $\gamma$  and  $\lambda$ ,<sup>21)</sup> but we will not discuss this issue in this paper.

In the following subsections, numerical solutions are presented in various dimensions. Before doing that, let us consider the analytical solution. It can be confirmed that the basic

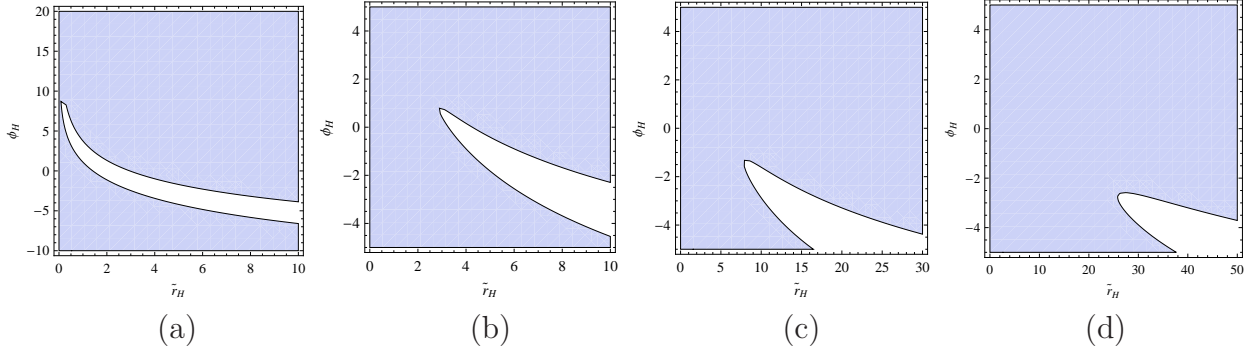


Fig. 1. The regions where Eq. (3.4) has real roots of  $\phi'_H$  (shaded area) for  $k = 1$  and  $\tilde{\Lambda} = -1$  in (a)  $D = 4$ , (b)  $D = 5$ , (c)  $D = 6$ , and (d)  $D = 10$ . On the boundary  $\phi'_H$  degenerates. Only in these regions, regularity at the event horizon can be satisfied.

equations have the exact solution

$$\phi \equiv \phi_0, \quad \delta \equiv 0, \quad B = \tilde{b}_2 \tilde{r}^2 + 1, \quad (4.4)$$

where the parameters  $\tilde{b}_2$  and  $\phi_0$  are given in Eqs. (3.9) and (3.10). This is the AdS solution and the spacetime is regular everywhere. To our knowledge, this is the first example of the exact solution in the dilatonic Einstein-GB system. It is important to note that there is not such a kind of exact solution without cosmological constant. The effective potential of the dilaton field is composed of two parts, the GB term and the cosmological constant. This allows the dilaton field to have equilibrium point in the effective potential. Without cosmological constant, however, the effective potential has slopes everywhere, and  $\phi$  cannot be constant.

#### 4.1. $D = 4$ solution

First we present the black hole solutions for  $D = 4$ . From Eqs. (3.9) and (3.10), we see that the square of inverse AdS radius and the asymptotic value of the dilaton field are  $\tilde{b}_2 = 1/6$  ( $\tilde{\ell}_{AdS} = \sqrt{6}$ ) and  $\phi_0 = 0$ , respectively. We show  $\phi_H, \delta_H$  and  $\tilde{M}_0$  as functions of  $\tilde{r}_H$  in solid lines in Fig. 2.  $\phi_H$  is negative and less than that of the  $k = 0$  case for any horizon radius, and approaches the value  $\phi_H^{(k=0)} = -0.0985664$  in the  $k = 0$  case for large horizon radius (Fig. 2(a)). There is a forbidden region in the left side of the  $\phi_H$ - $\tilde{r}_H$  diagram in Fig. 1(a). Consequently, as the horizon radius becomes small, the value  $(\tilde{r}_H, \phi_H)$  hits the forbidden region, and the solution disappears for horizon radius smaller than the critical value  $\tilde{r}_H = 3.245$ . For this critical horizon radius, the second derivatives of the dilaton field  $\phi''$  and  $\delta'$  diverge at the horizon while  $B'_H$  and  $\delta_H$  are finite (Fig. 2(b)). This behavior is similar to the zero cosmological constant case discussed in Refs. [1), 8). Since the critical horizon radius is larger than the AdS radius  $\tilde{\ell}_{AdS} = \sqrt{6}$ , the horizon of every solution stays

outside AdS radius. The gravitational mass  $\tilde{M}_0$  is monotonic with respect to  $\tilde{r}_H$  (Fig. 2(c)). In the  $k = 0$  case,<sup>2)</sup>  $\tilde{M}_0$  was proportional to  $\tilde{r}_H^{D-1}$  by the scaling symmetry. In the present case, it is found that similar proportional relation is gradually realized for the large black holes (Fig. 2(d)).

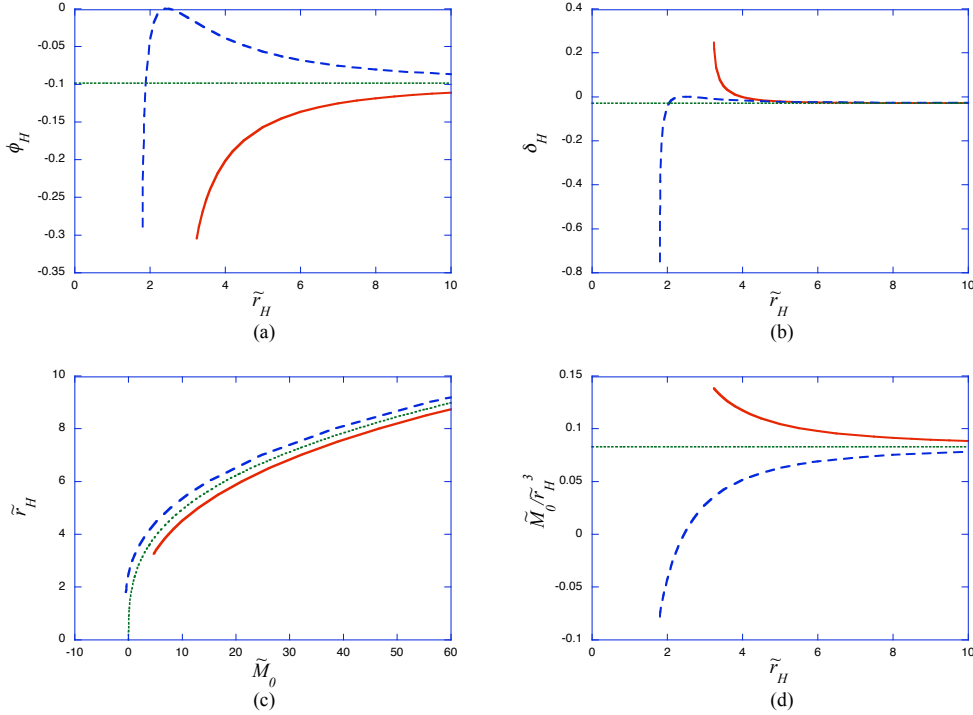


Fig. 2. Numerical values of the fields (a)  $\phi_H$  and (b)  $\delta_H$  at the horizon and the mass of the black hole (c)  $\tilde{M}_0$ - $\tilde{r}_H$  diagram in  $D = 4$ . (d) shows the scaled mass by horizon radius. For each figures,  $k = 1$  is in the solid (red) line,  $k = 0$  the dotted (green) line, and  $k = -1$  the dashed (blue) line. The AdS radius is  $\tilde{\ell}_{\text{AdS}} = \sqrt{6}$ , and the asymptotic value of the dilaton is  $\phi_0 = 0$ .

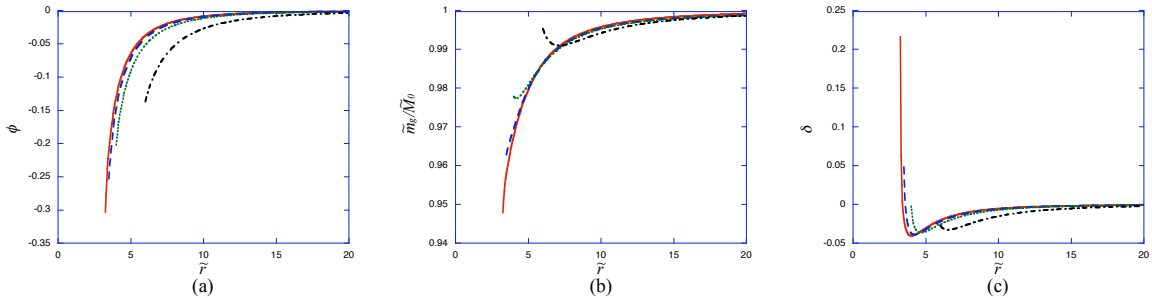


Fig. 3. Behaviors of (a) the dilaton field  $\phi(\tilde{r})$ , (b) the mass function  $\tilde{m}_g(\tilde{r})/\tilde{M}_0$  and (c) the lapse function  $\delta(\tilde{r})$  of the black hole solutions with  $k = 1$  in  $D = 4$ . The horizon radii and the masses are  $\tilde{r}_H = 3.25$ ,  $\tilde{M}_0 = 4.7322$  (solid line),  $\tilde{r}_H = 3.5$ ,  $\tilde{M}_0 = 5.5284$  (dashed line),  $\tilde{r}_H = 4.0$ ,  $\tilde{M}_0 = 7.4995$  (dotted line), and  $\tilde{r}_H = 6.0$ ,  $\tilde{M}_0 = 21.098$  (dot-dashed line).

The configurations of the fields in the black hole solutions are depicted in Fig. 3. The dilaton field increases monotonically to its asymptotic value  $\phi_0 = 0$ . The mass function increases monotonically for smaller black holes while it decreases near the event horizon for larger black holes. As the horizon radius approaches the critical value, the function  $\delta$  is finite but becomes steep around the event horizon.

#### 4.2. $D = 5$ solution

It follows from Eqs. (3-9) and (3-10) that the square of inverse AdS radius and the asymptotic value of the dilaton field are  $\tilde{b}_2 = 0.24346$  ( $\tilde{\ell}_{\text{AdS}} = 2.0267$ ) and  $\phi_0 = 2.84082$ , respectively. We show  $\phi_H, \delta_H$  and  $\tilde{M}_0$  as functions of  $\tilde{r}_H$  in Fig. 4. For the large black hole (naively for  $\tilde{r}_H \gtrsim \tilde{\ell}_{\text{AdS}}$ ),  $\phi_H$  is smaller than  $\phi_0$  as in the  $D = 4$  case (Fig. 4(a)).  $\phi_H$  approaches  $\phi_H^{(k=0)} = 2.767015$  in the  $\tilde{r}_H \rightarrow \infty$  limit. However, for the small black holes,  $\phi_H$  is larger than  $\phi_0$ . There is a forbidden region in the  $\phi_H$ - $\tilde{r}_H$  diagram in Fig. 1(b), and as the horizon radius becomes smaller, black hole solution disappears as in  $D = 4$ . However, in  $D = 5$ , the disappearance occurs before the parameters  $(\tilde{r}_H, \phi_H)$  hit the forbidden region in Fig. 1(b). For the critical horizon radius  $\tilde{r}_H = 0.805$ , below which there is no black hole solution, the horizon is regular but  $\phi''$  diverges at  $\tilde{r} = \tilde{r}_s \equiv 1.11896$ . By the field equations, the derivative of the metric functions  $B'$  and  $\delta'$  also diverge. The Kretschmann invariant

$$R^{\mu\nu\rho\sigma} R_{\mu\nu\rho\sigma} = (B'' - 3B'\delta' + 2B(\delta'^2 - \delta''))^2 + \frac{2(D-2)}{r^2}(B'^2 - 2BB'\delta' + 2B^2\delta'^2) + \frac{2(D-2)_3}{r^4}(k-B)^2, \quad (4.5)$$

diverges there, and hence the surface  $\tilde{r} = \tilde{r}_s$  is curvature singularity. These properties are quite different from the zero cosmological constant case,<sup>1)</sup> where the black hole solution exists for any horizon radius. It is possible, however, that these behaviors change if we change the parameter  $\gamma$ .<sup>21)</sup> It is interesting that the cosmological constant changes the small scale structure compared to the bare curvature radius defined by  $\tilde{\ell}^2 = -(D-1)_2/\tilde{\Lambda}$ , although it usually affects the properties of large structure. Relation between  $\tilde{M}_0$  and  $\tilde{r}_H$  is monotonic (Fig. 4(c)). It is also found that for the large horizon radius  $\tilde{M}_0$  is proportional to  $\tilde{r}_H^4$  (Fig. 4(d)).

We show the configurations of the fields in the black hole solutions in Fig. 5. For large black holes, the dilaton field increases monotonically to its asymptotic value  $\phi_0 = 2.84082$ . The mass function also increases monotonically. On the other hand, for small black holes, the dilaton field decreases rapidly around the event horizon and becomes smaller than  $\phi_0$ . Around these decreasing regions, the mass function varies violently. The dilaton field increases outside some radius towards its asymptotic value.

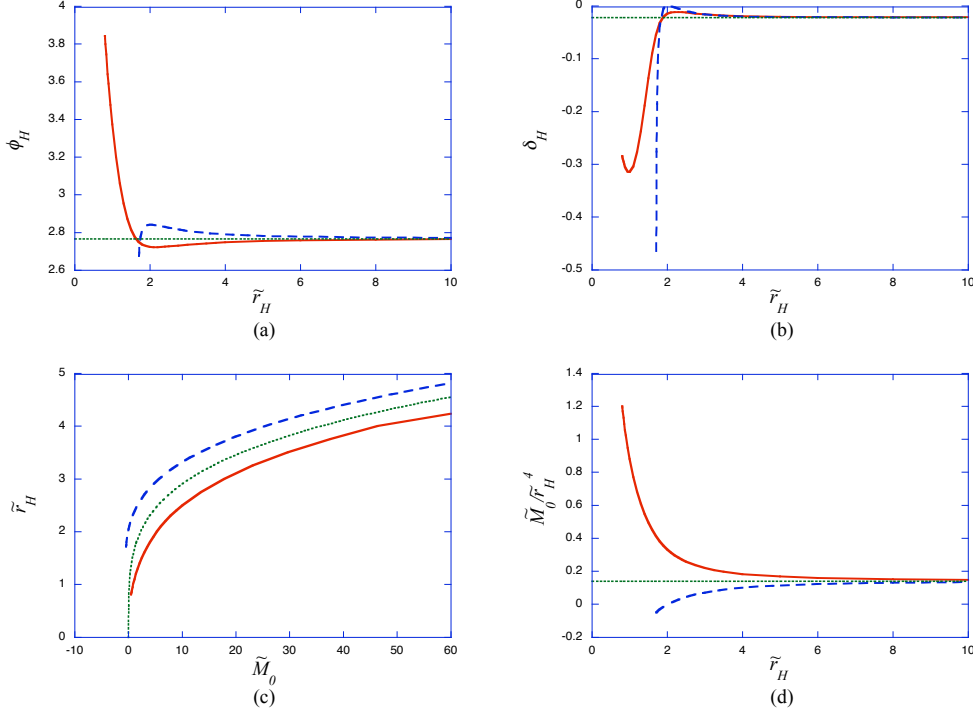


Fig. 4. Numerical values of the fields (a)  $\phi_H$  and (b)  $\delta_H$  at the horizon, and the mass of the black hole (c)  $\tilde{M}_0$ - $\tilde{r}_H$  diagram in  $D = 5$ . (d) shows the scaled mass by horizon radius. For each figure,  $k = 1$  is in the solid (red) line,  $k = 0$  the dotted (green) line, and  $k = -1$  the dashed (blue) line. The AdS radius is  $\tilde{\ell}_{\text{AdS}} = 2.0267$ , and the asymptotic value of the dilaton is  $\phi_0 = 2.84082$ .

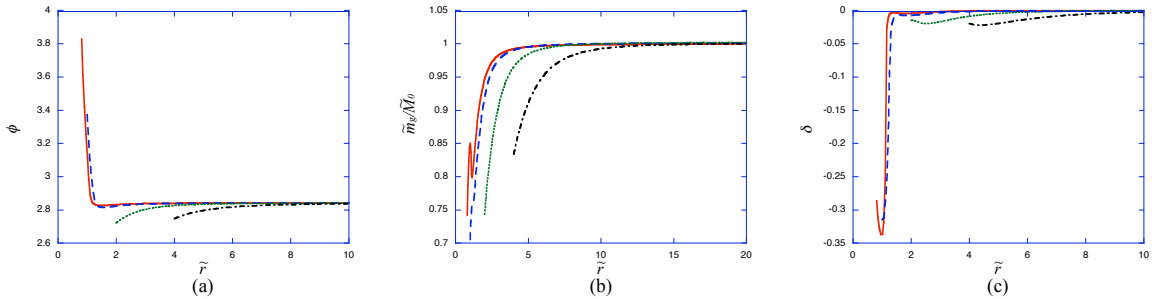


Fig. 5. Behaviors of (a) the dilaton field  $\phi(\tilde{r})$ , (b) the mass function  $\tilde{m}_g(\tilde{r})/\tilde{M}_0$  and (c) the lapse function  $\delta(\tilde{r})$  of the black hole solutions with  $k = 1$  in  $D = 5$ . The horizon radii and the masses are  $\tilde{r}_H = 0.81$ ,  $\tilde{M}_0 = 0.51273$  (solid line),  $\tilde{r}_H = 1.0$ ,  $\tilde{M}_0 = 0.88107$  (dashed line),  $\tilde{r}_H = 2.0$ ,  $\tilde{M}_0 = 5.3094$  (dotted line), and  $\tilde{r}_H = 4.0$ ,  $\tilde{M}_0 = 46.417$  (dot-dashed line).

#### 4.3. $D = 6$ solution

We see from Eqs. (3-9) and (3-10) that the square of inverse AdS radius and the asymptotic value of the dilaton field are  $\tilde{b}_2 = 0.248535$  ( $\tilde{\ell}_{\text{AdS}} = 2.0059$ ) and  $\phi_0 = 4.20868$ , respectively. We show  $\phi_H, \delta_H$  and  $\tilde{M}_0$  as functions of  $\tilde{r}_H$  in solid lines in Fig. 6. The qualitative

properties are the same as those in the  $D = 5$  case. For the large black hole ( $\tilde{r}_H \gtrsim \tilde{\ell}_{\text{AdS}}$ ),  $\phi_H$  is smaller than  $\phi_0$  (Fig. 6(a)).  $\phi_H$  approaches  $\phi_H^{(k=0)} = 4.15418$  in the  $\tilde{r}_H \rightarrow \infty$  limit. However, for the small black holes,  $\phi_H$  is larger than  $\phi_0$ . As the horizon radius becomes smaller, the black hole solution disappears at the critical radius  $\tilde{r}_H = 0.805$ . As is seen from Fig. 1(c), a forbidden region exists far below in the  $\phi_H$ - $\tilde{r}_H$  diagram. Hence the disappearance of solution is not due to hitting the forbidden region but due to diverging behavior of derivatives of the fields outside the event horizon as in  $D = 5$ . The gravitational mass  $\tilde{M}_0$  is monotonic with respect to  $\tilde{r}_H$  (Fig. 6(c)). It is found that for the large horizon radius  $\tilde{M}_0$  is proportional to  $\tilde{r}_H^5$  (Fig. 6(d)).

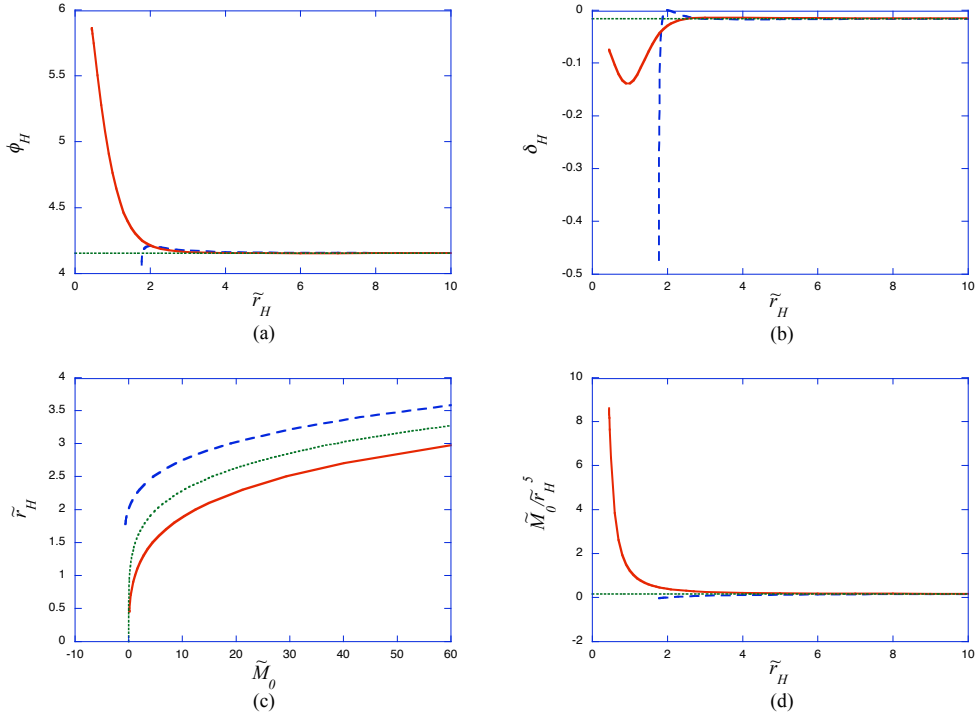


Fig. 6. Numerical values of the fields (a)  $\phi_H$  and (b)  $\delta_H$  at the horizon and the mass of the black hole (c)  $\tilde{M}_0$ - $\tilde{r}_H$  diagram in  $D = 6$ . (d) shows the scaled mass by horizon radius. For each figure,  $k = 1$  is in the solid (red) line,  $k = 0$  the dotted (green) line, and  $k = -1$  the dashed (blue) line. The AdS radius is  $\tilde{\ell}_{\text{AdS}} = 2.0059$ , and the asymptotic value of the dilaton is  $\phi_0 = 4.20868$ .

We show the configurations of the fields in the black hole solutions in Fig. 7. For large black holes, the dilaton field increases monotonically to its asymptotic value  $\phi_0 = 4.20868$ . The mass function also increases monotonically. On the other hand, for small black holes, the dilaton field decreases around the event horizon and increases towards its asymptotic value. There is a region where the mass function decreases.

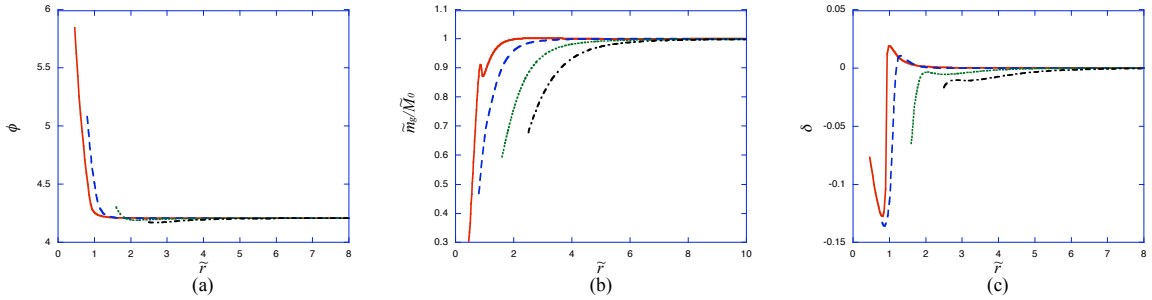


Fig. 7. Behaviors of (a) the dilaton field  $\phi(\tilde{r})$ , (b) the mass function  $\tilde{m}_g(\tilde{r})/\tilde{M}_0$  and (c) the lapse function  $\delta(\tilde{r})$  of the black hole solutions with  $k = 1$  in  $D = 6$ . The horizon radii and the masses are  $\tilde{r}_H = 0.46$ ,  $\tilde{M}_0 = 0.16813$  (solid line),  $\tilde{r}_H = 0.8$ ,  $\tilde{M}_0 = 0.63364$  (dashed line),  $\tilde{r}_H = 1.6$ ,  $\tilde{M}_0 = 5.6443$  (dotted line), and  $\tilde{r}_H = 2.5$ ,  $\tilde{M}_0 = 29.449$  (dot-dashed line).

#### 4.4. $D = 10$ solution

It follows from Eqs. (3.9) and (3.10) that the square of inverse AdS radius and the asymptotic value of the dilaton field are  $\tilde{b}_2 = 0.158862$  ( $\tilde{\ell}_{\text{AdS}} = 2.5089$ ) and  $\phi_0 = 6.30143$ , respectively. We show  $\phi_H, \delta_H$  and  $\tilde{M}_0$  as functions of  $\tilde{r}_H$  in solid lines in Fig. 8. For the large black hole ( $\tilde{r}_H \gtrsim 8$ ),  $\phi_H$  is smaller than  $\phi_0$  (Fig. 8(a)).  $\phi_H$  approaches  $\phi_H^{(k=0)} = 6.2916147$  in the  $\tilde{r}_H \rightarrow \infty$  limit. For the small black holes,  $\phi_H$  is larger than  $\phi_0$ . These qualitative properties are the same as those in  $D = 5$  and 6 case. However, as the horizon radius becomes smaller,  $\phi_H$  approaches  $\phi_0$ , and the solution continues to exist to zero horizon limit. This means that there is no critical horizon radius, and black hole solution exists for any horizon radius according to the numerical analysis. As is seen from Fig. 1(d), a forbidden region exists far below in the  $\phi_H$ - $\tilde{r}_H$  diagram. As the horizon radius becomes zero, variables  $\phi'$ ,  $\phi''$ , and  $\delta_H$  becomes zero. Hence the solution is connected to the regular AdS solution (4.4).\*) This is similar to the zero cosmological constant case.<sup>1)</sup> Relation between  $\tilde{M}_0$  and  $\tilde{r}_H$  is monotonic (Fig. 8(c)). It is found that for the large horizon radius  $\tilde{M}_0$  is proportional to  $\tilde{r}_H^9$  (Fig. 8(d)). On the other hand,  $\tilde{M}_0$  is proportional to  $\tilde{r}_H^5$  for the small horizon radius. These relations are the same as the non-dilatonic case.

We show the configurations of the fields in the black hole solutions in Fig. 9. For large black holes ( $\tilde{r}_H \gtrsim 8$ ), the dilaton field increases monotonically to its asymptotic value  $\phi_0 = 6.30143$ . The mass function also increases monotonically. On the other hand, for small black holes, the dilaton field decreases around the event horizon and increases towards its asymptotic value. The mass function also increases monotonically.

\*) This does not mean that the black hole solution changes to the regular AdS solution continuously through, for example, Hawking radiation.

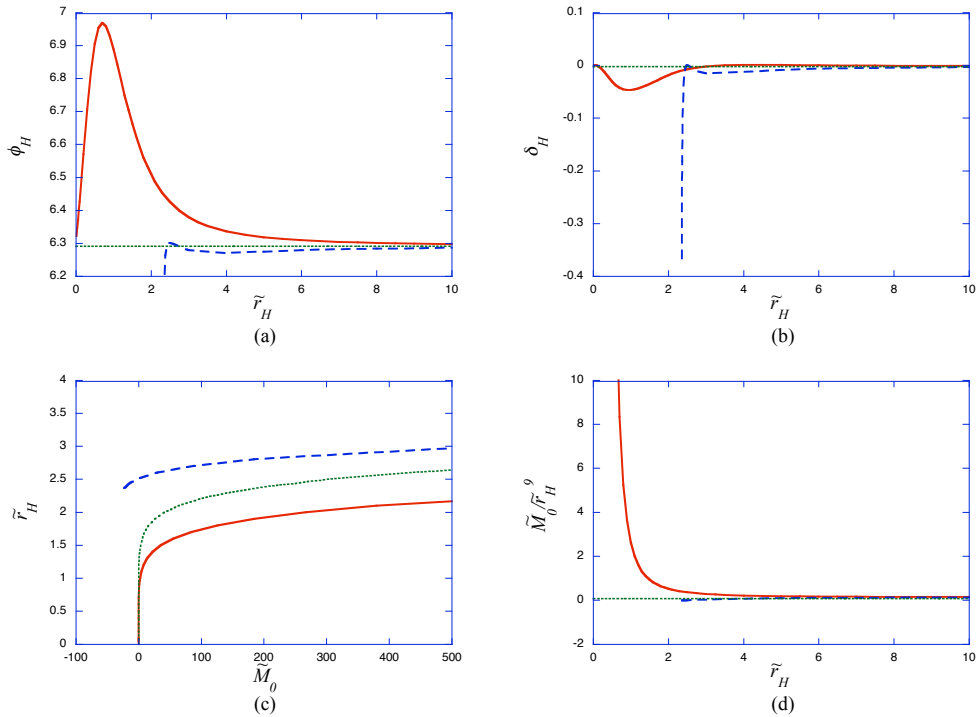


Fig. 8. Numerical values of the fields (a)  $\phi_H$  and (b)  $\delta_H$  at the horizon and the mass of the black hole (c)  $\tilde{M}_0$ - $\tilde{r}_H$  diagram in  $D = 10$ . (d) shows the scaled mass by horizon radius. For each figure,  $k = 1$  is in the solid (red) line,  $k = 0$  the dotted (green) line, and  $k = -1$  the dashed (blue) line. The AdS radius is  $\tilde{\ell}_{\text{AdS}} = 2.5089$ , and the asymptotic value of the dilaton is  $\phi_0 = 6.30143$ .

### §5. Hyperbolic black holes with $k = -1$

The procedure to calculate the black hole solutions are the same as that in  $k = 1$  case. It can be confirmed that the basic equations have the exact solution

$$\phi \equiv \phi_0, \quad \delta \equiv 0, \quad B = \tilde{b}_2 \tilde{r}^2 - 1. \quad (5.1)$$

where the parameters  $b_2$  and  $\phi_0$  are again given in Eqs. (3.9) and (3.10). This solution has an event horizon at  $\tilde{r} = 1/\sqrt{\tilde{b}_2}$ , which coincides with the AdS radius  $\tilde{\ell}_{\text{AdS}}$ . It follows from Eq. (3.14) that the mass of the black hole solution is  $\tilde{m}_g \equiv \tilde{M}_0 = 0$ . Hence this solution is the zero mass black hole. The center of the solution is not singular but regular.

The allowed parameter regions of  $(\phi'_H, \tilde{r})$  are shown in Figs. 10. Note that the forbidden regions appear in the larger values of  $\phi_H$  in contrast to  $k = 1$  case.

It turns out that qualitative properties of the black hole solutions do not depend on the spacetime dimensions. So, we present the solutions in  $D = 4 - 6$ , and 10 together.



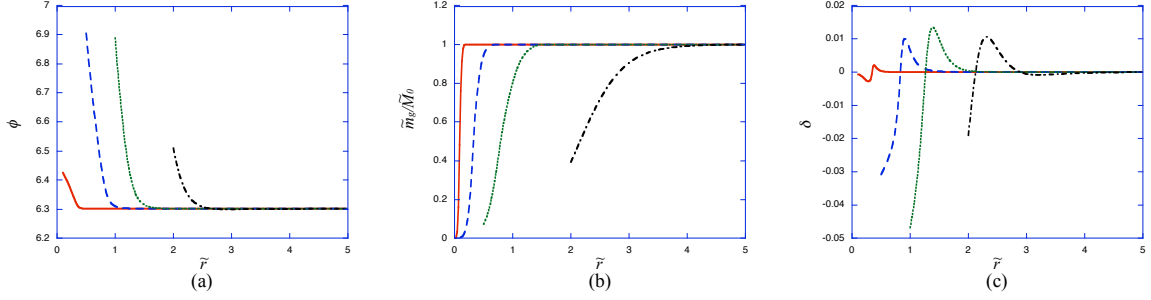


Fig. 9. Behaviors of (a) the dilaton field  $\phi(\tilde{r})$ , (b) the mass function  $\tilde{m}_g(\tilde{r})/\tilde{M}_0$  and (c) the lapse function  $\delta(\tilde{r})$  of the black hole solutions with  $k = 1$  in  $D = 10$ . The horizon radii and the masses are  $\tilde{r}_H = 0.01$ ,  $\tilde{M}_0 = 2.0898 \times 10^{-10}$  (solid line),  $\tilde{r}_H = 0.1$ ,  $\tilde{M}_0 = 1.9999 \times 10^{-5}$  (dashed line),  $\tilde{r}_H = 0.5$ ,  $\tilde{M}_0 = 5.5699 \times 10^{-2}$  (dotted line), and  $\tilde{r}_H = 2.0$ ,  $\tilde{M}_0 = 2.6667 \times 10^2$  (dot-dashed line).

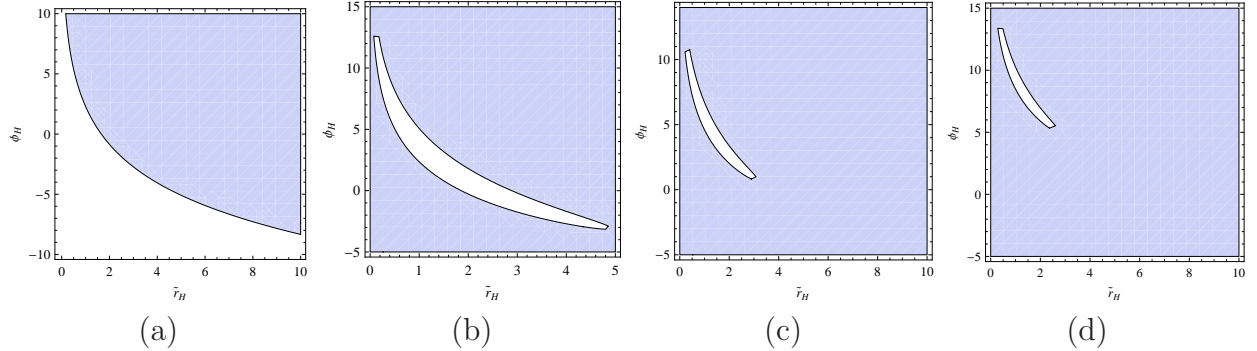


Fig. 10. The regions where Eq. (3.4) has real roots of  $\phi'_H$  (shaded area) for  $k = -1$  and  $\tilde{\Lambda} = -1$  in (a)  $D = 4$ , (b)  $D = 5$ , (c)  $D = 6$ , and (d)  $D = 10$ . On the boundary  $\phi'_H$  degenerates. Only in these regions, regularity at the event horizon can be satisfied.

The asymptotic value of the dilaton field  $\phi_0$  and the square of inverse AdS radius  $\tilde{b}_2 = \tilde{\ell}_{\text{AdS}}^{-2}$  are the same as those in the  $k = 1$  case for any dimensions. We show  $\phi_H$ ,  $\delta_H$  and  $\tilde{M}_0$  as functions of  $\tilde{r}_H$  in Figs. 2, 4, 6 and 8 for  $D = 4, 5, 6$  and 10, respectively, all in dashed lines. The solutions are classified by their horizon radius as  $\tilde{r}_H > \tilde{\ell}_{\text{AdS}}$  or  $\tilde{r}_H < \tilde{\ell}_{\text{AdS}}$ . For the large black holes ( $\tilde{r}_H > \tilde{\ell}_{\text{AdS}}$ ), the dilaton field at the horizon  $\phi_H$  is larger than that in the  $k = 0$  case, which is opposite to the  $k = 1$  case, but smaller than its asymptotic value  $\phi_0$ . As the  $\tilde{r}_H$  becomes large,  $\phi_H$  decreases, and approaches  $\phi_H^{(k=0)}$  in the  $\tilde{r}_H \rightarrow \infty$  limit. The gravitational mass  $\tilde{M}_0$  is monotonic with respect to  $\tilde{r}_H$ , and proportional to  $\tilde{r}_H^{D-1}$  for large  $\tilde{r}_H$ . It is smaller than those of the  $k = 0$  and  $+1$  with the same horizon radius.

The solution with  $\tilde{r}_H = \tilde{\ell}_{\text{AdS}}$  is given by Eq. (5.1), which is the zero mass black hole. In the non-dilatonic case, there are two branches of black hole solutions, i.e., the GR branch and the GB branch. In each of them, there is a zero mass black hole solution. In the dilatonic

case, however, there is only a single zero mass solution, which corresponds to the GR branch.

For the solution with  $\tilde{r}_H < \tilde{\ell}_{\text{AdS}}$ ,  $\phi_H$  decreases as the horizon radius becomes small, and the values  $(\tilde{r}_H, \phi_H)$  hit the forbidden region in Fig. 10. There is no solution for smaller horizon radius than the critical radius  $\tilde{r}_H = 1.807, 1.712, 1.777$  and  $2.364$ , for  $D = 4, 5, 6$  and  $10$ , respectively. For the critical horizon radius, the second derivative of the dilaton field  $\phi''$  diverges at the horizon. These are similar to the  $D = 4$  and  $k = 1$  case. In the non-dilatonic case, there is also a lower bound of the size of black hole solution in the GR-branch. In that case, two horizons (the black hole event horizon and the inner horizon) coincide, and the event horizons degenerate. In the present dilatonic case, however, the horizon becomes singular for the critical radius. The mass of these solution are negative.

We show the configurations of the fields in the black hole solutions in Fig. 11 – 14. For large black holes ( $\tilde{r}_H > \tilde{\ell}_{\text{AdS}}$ ), the dilaton field increases monotonically to its asymptotic value  $\phi_0$ . The mass function in  $D = 4$  decreases while those in higher dimensions  $D \geq 5$  increase monotonically. For  $\tilde{r}_H = \tilde{\ell}_{\text{AdS}}$ , the functions  $\phi$ ,  $m_g$  and  $\delta$  are constant. For small black holes ( $\tilde{r}_H < \tilde{\ell}_{\text{AdS}}$ ), the dilaton field decreases and becomes steep around the event horizon as  $\tilde{r}_H$  approaches its critical radius. The mass function in  $D = 4$  behaves monotonically while there is a range where the mass function changes its behavior in  $D \geq 5$ .

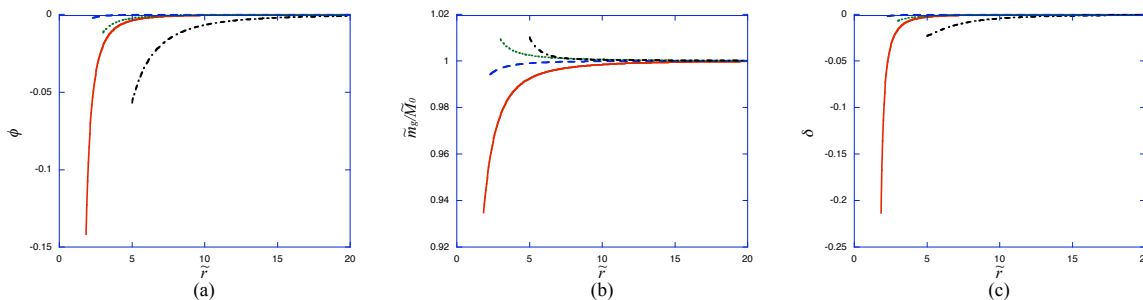


Fig. 11. Behaviors of (a) the dilaton field  $\phi$ , (b) the mass function  $\tilde{m}_g/\tilde{M}_0$  and (c) the lapse function  $\delta$  of the black hole solutions with  $k = -1$  in  $D = 4$ . The horizon radii and the masses are  $\tilde{r}_H = 1.85$ ,  $\tilde{M}_0 = -0.42504$  (solid line),  $\tilde{r}_H = 2.3$ ,  $\tilde{M}_0 = -0.13686$  (dashed line),  $\tilde{r}_H = 3.0$ ,  $\tilde{M}_0 = 0.74302$  (dotted line), and  $\tilde{r}_H = 5.0$ ,  $\tilde{M}_0 = 7.8371$  (dot-dashed line).

## §6. Conclusions and Discussions

We have studied the black hole solutions in dilatonic Einstein-GB theory with the negative cosmological constant. The cosmological constant introduces the Liouville type of potential for the dilaton field with a certain coupling. We have studied the spherically symmetric ( $k = 1$ ) and hyperbolically symmetric ( $k = -1$ ) spacetimes. The basic equations have some symmetries which are used to generate the black hole solutions with different horizon

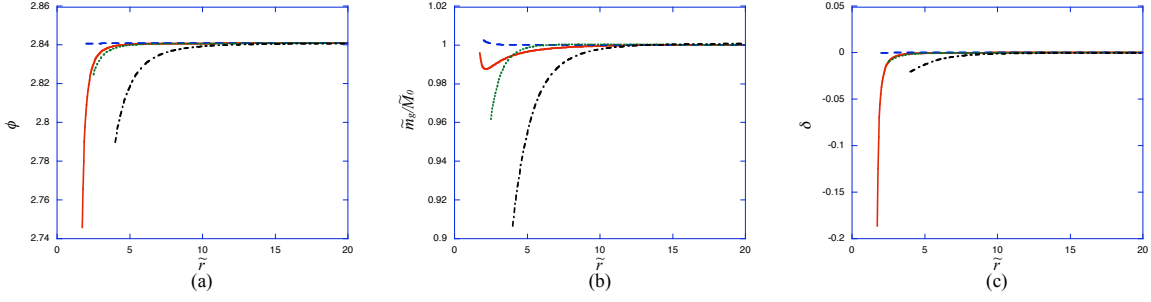


Fig. 12. Behaviors of (a) the dilaton field  $\phi$ , (b) the mass function  $\tilde{m}_g/\tilde{M}_0$  and (c) the lapse function  $\delta$  of the black hole solutions with  $k = -1$  in  $D = 5$ . The horizon radii and the masses are  $\tilde{r}_H = 1.73$ ,  $\tilde{M}_0 = -0.40774$  (solid line),  $\tilde{r}_H = 2.0$ ,  $\tilde{M}_0 = -5.2196 \times 10^{-2}$  (dashed line),  $\tilde{r}_H = 2.5$ ,  $\tilde{M}_0 = 1.6951$  (dotted line), and  $\tilde{r}_H = 4.0$ ,  $\tilde{M}_0 = 25.549$  (dot-dashed line).

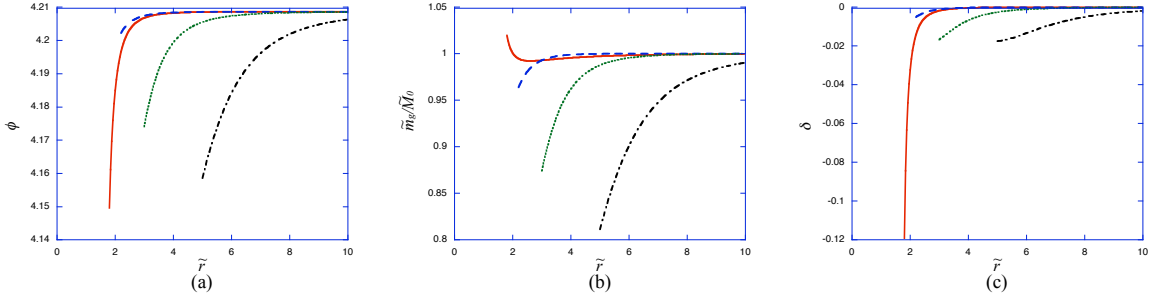


Fig. 13. Behaviors of (a) the dilaton field  $\phi$ , (b) the mass function  $\tilde{m}_g/\tilde{M}_0$  and (c) the lapse function  $\delta$  of the black hole solutions with  $k = -1$  in  $D = 6$ . The horizon radii and the masses are  $\tilde{r}_H = 1.82$ ,  $\tilde{M}_0 = -0.51938$  (solid line),  $\tilde{r}_H = 2.2$ ,  $\tilde{M}_0 = 1.1209$  (dashed line),  $\tilde{r}_H = 3.0$ ,  $\tilde{M}_0 = 19.097$  (dotted line), and  $\tilde{r}_H = 5.0$ ,  $\tilde{M}_0 = 4.0156 \times 10^2$  (dot-dashed line).

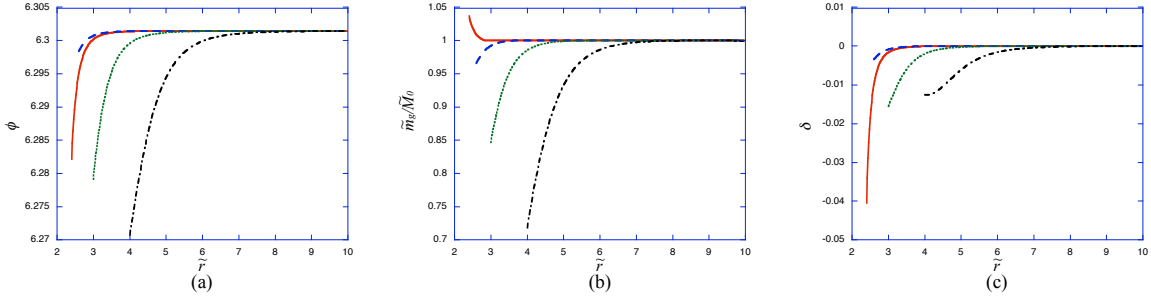


Fig. 14. Behaviors of (a) the dilaton field  $\phi$ , (b) the mass function  $\tilde{m}_g/\tilde{M}_0$  and (c) the lapse function  $\delta$  of the black hole solutions with  $k = -1$  in  $D = 10$ . The horizon radii and the masses are  $\tilde{r}_H = 2.4$ ,  $\tilde{M}_0 = -1.8787 \times 10^1$  (solid line),  $\tilde{r}_H = 2.6$ ,  $\tilde{M}_0 = 3.0737 \times 10^1$  (dashed line),  $\tilde{r}_H = 3.0$ ,  $\tilde{M}_0 = 5.5498 \times 10^2$  (dotted line), and  $\tilde{r}_H = 4.0$ ,  $\tilde{M}_0 = 1.7587 \times 10^4$  (dot-dashed line).

radii and the cosmological constants.

The black hole solution should have a regular event horizon and be singularity free in the outer region. By the asymptotic expansion at infinity, where the spacetime approaches

AdS spacetime, the power decaying rate of the fields are estimated. We have imposed the condition that the “mass” of the dilaton field satisfies the BF bound, which guarantees the stability of the vacuum solution. By this condition, the values of the dilaton coupling constant and the parameter of the Liouville potential are constrained. For a typical choice of the parameters and boundary conditions, we were able to construct AdS black hole solutions in various dimensions numerically.

We have chosen  $\gamma = 1/2$  and  $\lambda = 1/3$  for the actual numerical analysis. The black hole solutions are constructed in  $D = 4, 5, 6$  and 10. We have checked that the dilaton field climbs up its potential slope and takes constant values at infinity. The field equations have exact solutions, i.e., regular AdS solution for  $k = 1$  and a massless black hole solution for  $k = -1$ . The nontrivial solutions are obtained numerically in  $D = 4 - 6$  and 10 dimensional spacetimes.

For spherically symmetric solution ( $k = 1$ ), there is the critical horizon radius below which no solution exists in  $D = 4 - 6$ . In  $D = 4$ , The field functions diverge at the horizon for solution with the critical horizon radius. In  $D = 5$  and 6, the event horizon of the critical solution is regular but the derivatives of fields diverge at some radius outside the event horizon. In  $D = 10$ , however, there is not such lower bound of the horizon radius but the solution continues to exist to zero horizon size. In the large black hole limit ( $\tilde{r}_H \rightarrow \infty$ ), the solution approaches the planar symmetric one ( $k = 0$ ), and the mass is proportional to  $\tilde{r}_H^{D-1}$ .

For hyperbolically symmetric solution ( $k = -1$ ), the solutions are classified by their horizon radius as  $\tilde{r}_H > \tilde{\ell}_{\text{AdS}}$  or  $\tilde{r}_H < \tilde{\ell}_{\text{AdS}}$ . As the  $\tilde{r}_H$  becomes large,  $\phi_H$  decreases, and approaches  $\phi_H^{(k=0)}$  in the  $\tilde{r}_H \rightarrow \infty$  limit. The gravitational mass  $\tilde{M}_0$  is monotonic with respect to  $\tilde{r}_H$ , and is proportional to  $\tilde{r}_H^{D-1}$ . The solution with  $\tilde{r}_H = \tilde{\ell}_{\text{AdS}}$  is given by Eq. (5.1), which is the zero mass black hole. For the solution with  $\tilde{r}_H < \tilde{\ell}_{\text{AdS}}$ ,  $\phi_H$  decreases as the horizon radius becomes small. There is the critical horizon radius in all dimensions, and the fields of the critical solution diverge at the horizon. The mass of these solution are negative.

There are some remaining issues left for future works. One of them is the thermodynamics of our black holes. The Hawking temperature is given by the periodicity of the Euclidean time on the horizon as

$$\begin{aligned} \tilde{T}_H &= \frac{e^{-\delta_H}}{4\pi} B'_H \\ &= \frac{e^{-\delta_H}}{4\pi h_H} \left[ \frac{(D-3)k}{\tilde{r}_H} + \frac{(D-3)_5 k^2}{\tilde{r}_H^2} e^{-\gamma\phi_H} - \frac{\tilde{r}_H \tilde{\Lambda} e^{\lambda\phi_H}}{D-2} \right]. \end{aligned} \quad (6.1)$$

In the case of GB gravity, the entropy is not obtained by a quarter of the area of the event horizon. Along the definition of entropy in Ref. 25), which originates from the Noether

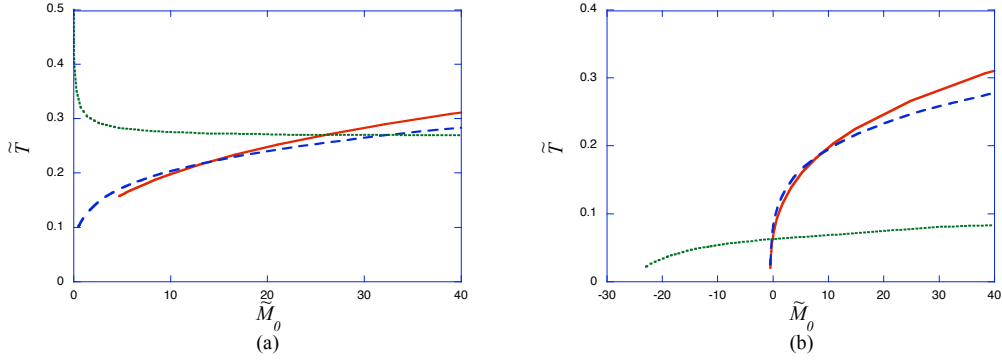


Fig. 15. Temperature of the black hole solution with (a)  $k = 1$  and (b)  $k = -1$  in  $D = 4$  (solid line),  $D = 5$  (dashed line), and  $D = 10$  (dotted line).

charge associated with the diffeomorphism invariance of the system, we obtain

$$\tilde{S} = \frac{\tilde{r}_H^{D-2} \Sigma_k}{4} \left[ 1 + 2(D-2)_3 \frac{k e^{-\gamma \phi_H}}{\tilde{r}_H^2} \right] - \tilde{S}_{min}, \quad (6.2)$$

where  $S_{min}$  is added to make the entropy non-negative.<sup>26)</sup> The temperatures of the black holes are plotted in Fig. 15. In  $D = 10$ , the temperature of the black hole with  $k = 1$  diverges in the zero horizon radius limit while the other solutions have finite temperature even for the solutions with the critical horizon radius. For the solutions with  $k = 1$  in  $D = 4$  and the ones with  $k = -1$ , the critical horizon radius is determined by the reality of  $\phi'$  at horizon. At the horizon of the critical solution,  $\phi''$  diverges but  $B'$  and  $\delta$  are finite as discussed in § 4 and § 5. For the solutions with  $k = 1$  in  $D = 5$  and 6, the critical solutions are determined by the divergence of the second derivative of the dilaton field outside the horizon. This means that the horizon is regular. Hence for these solutions the temperature is finite.

Since the temperature of the black hole is non-zero for all mass range, we expect that our black holes will not stop evaporating process via Hawking radiation. Then the following fates are considered: (i) The black hole becomes small and the horizon radius reaches the critical radius. Then the naked singularity appears. (ii) The solution is deformed to less symmetric (non-spherically/hyperbolically symmetric) one. (iii) Other higher curvature correction terms become important and lead to different fates from the present analysis. Since the curvatures diverge for the critical solution, the case (iii) seems plausible. However we have to study the evaporation process more carefully, and let us examine the process in the present model.

Recall that the temperature of the extreme black hole with  $\gamma > \sqrt{2}$  in the Einstein-Maxwell-Dilaton system is infinite.<sup>3),4)</sup> Although the naive expectation is that this leads to an infinite emission rate, Holzhey and Wilczek showed that the potential, through which

created particles travel away to infinity, grows infinitely high in the extreme limit, and then it is expected that the emission rate could be suppressed to a finite value<sup>27)</sup> although the detailed analysis leads to the different conclusion.<sup>28)</sup> In our case, if the potential barrier becomes infinitely large, the emission rate might be suppressed to zero even though the temperature of the black hole remains finite. Then evaporation may stop and the black hole cannot reach the critical solution. To study this possibility, we have to calculate the potential barrier for the field of evaporating particles in the background of our new solutions.

Here we examine a free neutral massless scalar field  $\Phi$ , which obeys the Klein-Gordon equation:

$$\square \Phi = 0. \quad (6.3)$$

We expand the scalar field in harmonics and study the mode

$$\Phi = \frac{\chi(\tilde{r})}{\tilde{r}^{(D-2)/2}} Y_{lm}(\psi) e^{-i\omega t}. \quad (6.4)$$

Eq. (6.3) becomes separable, and the radial equation reduces to

$$\left[ \frac{d^2}{d\tilde{r}^{*2}} + \omega^2 - V^2(\tilde{r}) \right] \chi(\tilde{r}^*) = 0, \quad (6.5)$$

where  $\tilde{r}^*$  is the tortoise coordinate defined as

$$\frac{d}{d\tilde{r}^*} = B e^{-\delta} \frac{d}{d\tilde{r}} \quad (6.6)$$

and  $V^2(r)$  is the potential;

$$V^2(\tilde{r}) = \frac{(D-2)B e^{-2\delta}}{2\tilde{r}^2} \left[ l(l+D-3) + \tilde{r}B' - \tilde{r}\delta'B + \frac{D-4}{2} \right]. \quad (6.7)$$

For the critical solutions with  $k = 1$  in  $D = 4$  and the ones with  $k = -1$ , the curvature singularity appears at the horizon, where  $\delta'$  diverges but  $B = 0$ . Hence the potential is finite there. As a result, the evaporating process does not stop. On the other hand, for the solutions with  $k = 1$  in  $D = 5$  and 6, the potential of the near critical black hole is plotted in Fig. 16. The potential forms sharp barrier and it may stop the evaporation and give a regular remnant.

To study the evolution of the black hole, deeper consideration should be necessary including the higher order corrections and potential barrier at AdS infinity. This is left for future study. A related issue is that the existence or non-existence of these critical solutions seems to depend on the value of the parameter  $\gamma$  and  $\lambda$ .<sup>21)</sup> This is expected because the dilaton significantly affects the solutions if the dilaton coupling is stronger. Stability and cosmological implications of these solutions should also be studied.<sup>29)</sup> The solution for

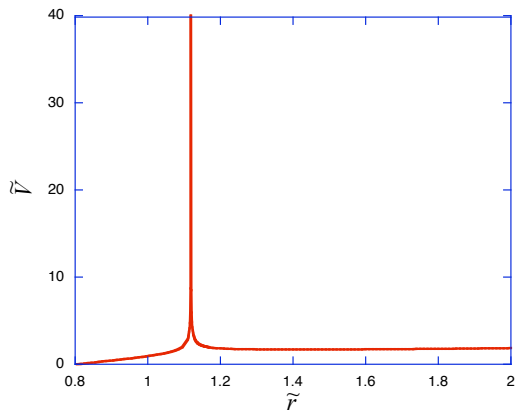


Fig. 16. Potential function of the free massless scalar field around the near critical black hole solution with  $k = 1$  and  $\tilde{r}_H = 0.805$  in  $D = 5$ . There is a sharp barrier outside the event horizon.

the positive cosmological constant is also a subject of future study, which will be reported elsewhere. Finally we hope that our asymptotically AdS black hole solutions are useful for examining properties of field theories via AdS/CFT correspondence.

### Acknowledgements

We would like to thank Z. K. Guo for collaboration on the earlier papers, and Kei-ichi Maeda for valuable discussions. The work of N.O. was supported in part by the Grant-in-Aid for Scientific Research Fund of the JSPS Nos. 20540283 and 06042, and also by the Japan-U.K. Research Cooperative Program.

### References

- 1) Z. K. Guo, N. Ohta and T. Torii, Prog. Theor. Phys. **120** (2008) 581 [arXiv:0806.2481 [gr-qc]].
- 2) Z. K. Guo, N. Ohta and T. Torii, Prog. Theor. Phys. **121** (2009) 253 [arXiv:0811.3068 [gr-qc]].
- 3) G. W. Gibbons and K. Maeda, Nucl. Phys. **B298** (1988) 741.
- 4) D. Garfinkle, G. T. Horowitz, and A. Strominger, Phys. Rev. D **43** (1991) 3140.
- 5) D. J. Gross and J. H. Sloan, Nucl. Phys. B **291** (1987) 41;  
M. C. Bento and O. Bertolami, Phys. Lett. B **368** (1996) 198.
- 6) P. Kanti, N. E. Mavromatos, J. Rizos, K. Tamvakis and E. Winstanley, Phys. Rev. D **54** (1996) 5049 [arXiv:hep-th/9511071].

- 7) S. O. Alexeev and M. V. Pomazanov, Phys. Rev. D **55** (1997) 2110 [arXiv:hep-th/9605106].
- 8) T. Torii, H. Yajima and K. Maeda, Phys. Rev. D **55** (1997) 739 [arXiv:gr-qc/9606034].
- 9) C. M. Chen, D. V. Gal'tsov and D. G. Orlov, Phys. Rev. D **75** (2007) 084030 [arXiv:hep-th/0701004].
- 10) C. M. Chen, D. V. Gal'tsov and D. G. Orlov, arXiv:0809.1720 [hep-th].
- 11) D. G. Boulware and S. Deser, Phys. Rev. Lett. **55** (1985) 2656.
- 12) J. T. Wheeler, Nucl. Phys. B **268** (1986) 737;  
D. L. Wiltshire, Phys. Lett. B **169** (1986) 36;  
R. C. Myers and J. Z. Simon, Phys. Rev. D **38** (1988) 2434;  
G. Giribet, J. Oliva and R. Troncoso, JHEP **0605** (2006) 007 [arXiv:hep-th/0603177];  
R. G. Cai and N. Ohta, Phys. Rev. D **74** (2006) 064001 [arXiv:hep-th/0604088].  
For reviews and references, see C. Garraffo and G. Giribet, arXiv:0805.3575 [gr-qc] and C. Charmousis, arXiv:0805.0568 [gr-qc].
- 13) R. G. Cai, Phys. Rev. D **65** (2002) 084014 [arXiv:hep-th/0109133].
- 14) L. Alvarez-Gaume, P. H. Ginsparg, G. W. Moore and C. Vafa, Phys. Lett. B **171** (1986) 155.
- 15) J. Polchinski, "String theory," *Cambridge Univ. Pr.* (1998).
- 16) R. G. Cai, Z. Y. Nie, N. Ohta and Y. W. Sun, arXiv:0901.1421 [hep-th].
- 17) S. J. Poletti and D. L. Wiltshire, Phys. Rev. D **50** (1994) 7260 [Erratum-ibid. D **52** (1995) 3753] [arXiv:gr-qc/9407021];  
S. J. Poletti, J. Twamley and D. L. Wiltshire, Phys. Rev. D **51** (1995) 5720 [arXiv:hep-th/9412076].
- 18) K. C. K. Chan, J. H. Horne and R. B. Mann, Nucl. Phys. B **447** (1995) 441 [arXiv:gr-qc/9502042].
- 19) C. Charmousis, Class. Quant. Grav. **19** (2002) 83 [arXiv:hep-th/0107126].
- 20) K. Bamba, Z. K. Guo and N. Ohta, Prog. Theor. Phys. **118** (2007) 879 [arXiv:0707.4334 [hep-th]].
- 21) K. Maeda, N. Ohta and Y. Sasagawa, in preparation.
- 22) M. Henneaux and C. Teitelboim, Comm. Math. Phys. **98** (1985) 391.
- 23) P. Breitenlohner and D. Z. Freedman, Annals Phys. **144** (1982) 249.
- 24) T. Hertog and K. Maeda, JHEP **0407** (2004) 051 [arXiv:hep-th/0404261].
- 25) R. M. Wald, Phys. Rev. D **48** (1993) 3427 [arXiv:gr-qc/9307038];  
V. Iyer and R. M. Wald, Phys. Rev. D **50** (1994) 846 [arXiv:gr-qc/9403028].
- 26) T. Clunan, S. F. Ross and D. J. Smith, Class. Quant. Grav. **21** (2004) 3447 [arXiv:gr-



- qc/0402044]. See also M. Cvetič, S. Nojiri and S. D. Odintsov, Nucl. Phys. B **628** (2002) 295 [arXiv:hep-th/0112045].
- 27) C. F. E. Holzhey and F. Wilczek, Nucl. Phys. B **380** (1992) 447 [arXiv:hep-th/9202014].
- 28) J. Koga and K. Maeda, Phys. Rev. D **52** (1995) 7066 [arXiv:hep-th/9508029].
- 29) P. Pani and V. Cardoso, arXiv:0902.1569 [gr-qc].